The Rate of Dissipation of Turbulent Energy in the Upper Layer of the Ocean

V. S. BELYAEV, M. M. LUBIMTZEV AND R. V. OZMIDOV

P. P. Shirshov Institute of Oceanology, USSR Academy of Sciences, Moscow

(Manuscript received 14 May 1974, in revised form 11 March 1975)

ABSTRACT

Based on empirical data for the upper layer of the ocean, estimates of the rate of turbulent energy dissipation $\bar{\epsilon}$ are obtained. The calculations of $\bar{\epsilon}$ were made in four ways. The slope of the spectra $E_1^{(\epsilon)}(K)$ of fluctuations of ϵ determines the universal constant of the refined theory of the locally isotropic turbulence $\mu=0.56\pm0.11$. The large departure from normality of the ϵ distributions indicates the strong intermittency of the small-scale fluctuations of the current velocity. Using the slopes of the high-order structure functions $D_P(r)=\langle|u(x+r)-u(x)|^P\rangle$, $P=1, 2, \ldots, 8$, the universal constants μ_P characterizing the momenta of the rate of the dissipation of turbulent energy ϵ_r averaged over the sphere with a radius $r/2$ are determined.

1. Introduction

The rate of turbulent kinetic energy dissipation into heat

$$\epsilon(\mathbf{x},t)=\frac{\nu}{2}\sum_{i,j=1}^{3}\left(\frac{\partial u_i}{\partial x_j}+\frac{\partial u_j}{\partial x_i}\right)^2, \qquad (1)$$

where u_i are velocity components in Cartesian coordinates x_i and ν the kinematic coefficient of molecular viscosity, can be considered the most important characteristic of turbulence. In the case of locally isotropic turbulence one can obtain from (1) the mean value of ϵ

$$\bar{\epsilon}=15\nu\overline{\left(\frac{\partial u}{\partial x}\right)^2}, \qquad (2)$$

where $u=u_1$ is the longitudinal component of the current velocity and bars indicate averages.

As is known, in Kolmogorov's theory of locally isotropic turbulence, $\bar{\epsilon}$ and ν are considered determining parameters. Refinements of this theory, taking into account the random character of the $\epsilon(\mathbf{x},t)$ field in space and time, have been suggested by Kolmogorov (1962) and Obukhov (1962). Accordingly, statistical characteristics of small-scale turbulence should be determined from *local*, but *not* mean, values of the dissipation ϵ. It has also been suggested that $\log_e\epsilon_r$ is distributed normally with dispersion, i.e.,

$$\sigma^2_{\log_e\epsilon_r}(\mathbf{x},t)=A(\mathbf{x},t)+\mu\log_e(L/r). \qquad (3)$$

Here ϵ_r is the value of the dissipation rate averaged in space over a spherical volume with radius $r/2$, where r is in the inertial subrange, $A(\mathbf{x},t)$ depends on the macrostructure of the turbulence field, L is the external scale of the flow, and μ a universal constant. Yaglom (1966) has shown that in the inertial subrange, the spectrum $E^{(\epsilon)}(k)$ of the ϵ_r fluctuations is proportional to K^n where $n=-1+\mu$.

The present paper presents results from calculations of ϵ and μ as well as the high-order structure functions of the velocity field in the ocean, using experimental data obtained during cruise 9 of the research vessel *Akademik Kurchatov* (Atlantic Ocean, 1971) and cruise 7 of *Dmitry Mendeleev* (Indian Ocean, 1972). These measurements were made with a short-response velocity sensor towed behind the ship. Because of a large towing velocity of about 3–4 m s^{-1}, this permits use of the Taylor hypothesis of "frozen turbulence" to transform time characteristics to space characteristics. Longitudinal velocity components were sensed with hydroresistor fluctuating velocity meters of the thermo-anemometric type with a threshold sensitivity of 0.5 mm s^{-1} and space resolution of 1 mm. The frequency bandpass of the measuring system (sensor, cable, and readout instrumentation) ranges within $f_{\min}=0.5$ and $f_{\max}=150$ Hz. Therefore, the digitized interval of analogue signal readings was chosen as $\frac{1}{2}f_{\max}=(1/300)$s.

2. Calculations of the $\bar{\epsilon}$, μ and ϵ spectra

The initial series of data for fluctuating velocities were transformed into new series of squared differences of longitudinal velocities at adjoining instants of time $(\Delta_n u)^2=[u(t_{n+1})-u(t_n)]$ and processed statistically on a computer.

Then the quantity $\bar{\epsilon}$ was evaluated from the formula

$$\bar{\epsilon}_1=\frac{15\nu}{V_{\rm rel}^2}\overline{\left(\frac{\Delta_n u}{\Delta t}\right)^2}, \qquad (4)$$

TABLE 1. Results of calculations based on the experimental data obtained on a given area of the Atlantic Ocean.

H (m)	$\tilde{\epsilon}_1$ (cm² s⁻³)	$\tilde{\epsilon}_2$ (cm² s⁻³)	$\tilde{\epsilon}_3$ (cm² s⁻³)	$\sigma_{\tilde{\epsilon}_1}$ (cm² s⁻³)	$\sigma_{\tilde{\epsilon}_2}$ (cm² s⁻³)	$\sigma_{\tilde{\epsilon}_3}$ (cm² s⁻³)	k_s	k_f	μ
36	9.5×10^{-2}	6.3×10^{-2}	1.5×10^{-1}	7.7×10^{-3}	7.2×10^{-3}	1.8×10^{-2}	3.86	32.89	0.43
52	1.6×10^{-1}	1.1×10^{-1}	3.4×10^{-1}	2.9×10^{-2}	2.2×10^{-1}	1.2×10^{-1}	5.56	62.97	0.62
73	7.7×10^{-2}	4.9×10^{-2}	1.1×10^{-1}	1.2×10^{-2}	1.2×10^{-2}	4.6×10^{-2}	2.41	8.59	0.71
90	1.8×10^{-1}	1.3×10^{-1}	3.9×10^{-1}	4.0×10^{-2}	3.6×10^{-2}	1.0×10^{-1}	2.63	11.88	0.63
110	1.8×10^{-1}	1.1×10^{-1}	2.4×10^{-1}	2.4×10^{-2}	2.1×10^{-2}	4.8×10^{-2}	2.09	6.22	0.51
140	3.7×10^{-2}	2.7×10^{-2}	3.7×10^{-2}	8.1×10^{-3}	6.4×10^{-3}	—	16.20	38.05	0.46

where V_{rel} is the velocity of the sensor relative to the water. The replacement of the partial differential in (2) by finite differences in (4) does not cause substantial error in the evaluation of (2), since in an analogue signal of velocity there are few if any components with frequency higher than $f_{max}=\frac{1}{2}\Delta t$. In addition, $\bar{\epsilon}$ can also be evaluated with the help of the integral relationship

$$\bar{\epsilon}_2=\int_0^\infty k^2E_1(k)dk, \tag{5}$$

where k is the wavenumber and $E_1(k)$ the one-dimensional spectral density of the longitudinal velocity. Since the functions $k^2E_1(k)$ usually had a distinct maximum in the bandpass of the measuring system, the evaluation of $\bar{\epsilon}$ in the spectral band 0.5–150 Hz, as used here, can be considered quite accurate. Finally, it has been suggested by Stewart and Grant (1962) that a value of $\bar{\epsilon}$ can be deduced by comparing the universal spectral curve with the experimental points $E_1(k)$.

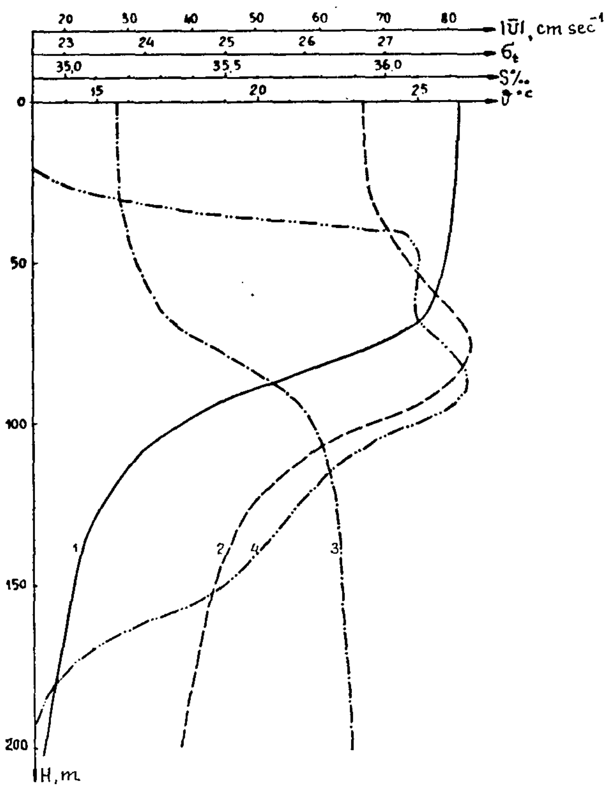

FIG. 1. Vertical distribution of temperature (1), salinity (2), density σ_t (3), and absolute value of flow velocity (4) based on standard hydrographic observations.

Table 1 presents the results of calculations using data obtained in a specific area of the Atlantic Ocean for the averaged hydrographic conditions shown in Fig. 1. The first column of Table 1 gives the depths of the different levels of measurement. At each level about 10 series with $N=2100$ readings were processed. The next three columns present the mean rates of dissipation of turbulent energy, determined with the help of the three methods described above. Tildes above $\bar{\epsilon}$ indicate averaged values for each level. The values of $\bar{\epsilon}$ obtained by the different methods coincide in order of magnitude. The next three columns contain the mean-square deviations $\sigma_{\bar{\epsilon}_i}$ of $\bar{\epsilon}$ from the averaged values $\tilde{\epsilon}_i$ ($i=1, 2, 3$) for each level.

The next two columns give the skewness k_s and flatness k_f for individual realizations of the random quantity ϵ. Large values of k_f indicate the existence of strong intermittency of ϵ_1 and of the small-scale velocity field in the ocean.

The last column gives values of the universal constant μ, determined from the slope of the spectrum $E_1^{(\epsilon_1)}(k)$ on a bi-logarithmic plot. These values lie between 0.43 and 0.71 with mean value 0.56 and mean square deviation 0.11. For atmospheric data, the quantity μ is approximately equal to 0.5.

In a number of cases, empirical spectra, without a clearly pronounced inertial subrange, can be approximated by Monin's (1962) theoretical curve in the transitional buoyancy-inertial range, which also permits evaluation of the dissipation rate. Such calculations yield for $\bar{\epsilon}$ values of 10^{-2} to 10^{-1} cm² s⁻³.

For an evaluation of the other statistical characteristics of $\epsilon(\mathbf{x},t)$, the series $(\epsilon_1)_n=15\nu(\Delta_n u/\Delta t)^2/V_{rel}^2$ have been employed. Fig. 2 shows the dimensionless spectra $E_1^{(\epsilon_1)}(k)/\eta\sigma_{\epsilon_1}^2$, where $\eta=(\nu^3/\bar{\epsilon}_1)^{\frac{1}{4}}$ is the internal scale of turbulence and $\sigma_{\epsilon_1}^2$ is the dispersion of the series $(\epsilon_1)_n$; different levels of measurement are identified by different symbols. The non-dimensional wavenumbers vary in the interval 6.0×10^{-3} to 2.4×10^{-1}. On the figure, the 95% confidence limits of the individual spectra are indicated by the vertical bar. The slope of

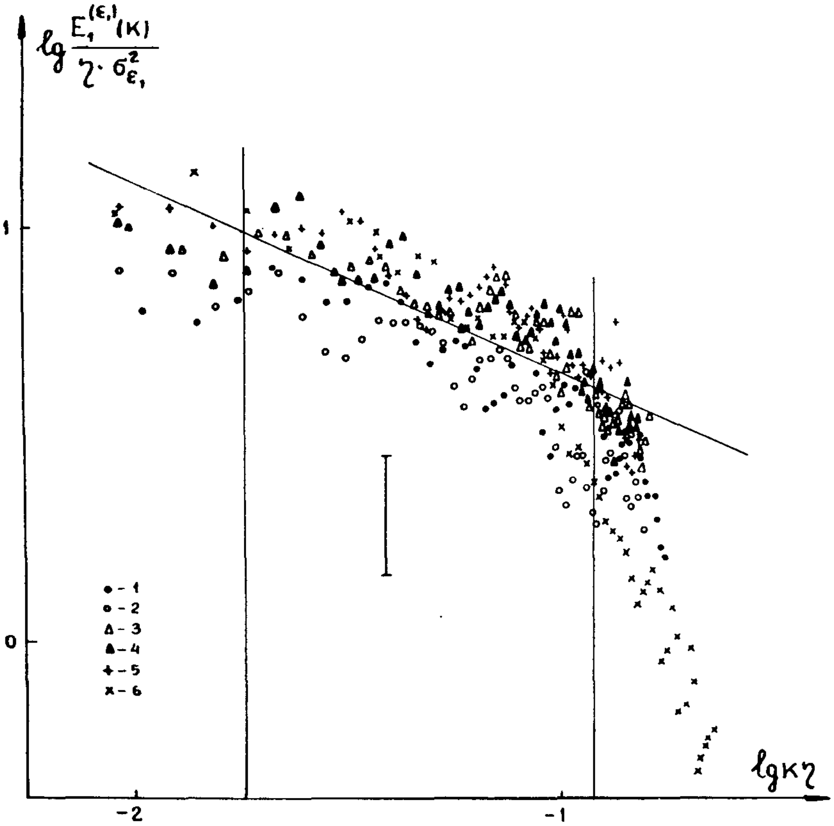

FIG. 2. Non-dimensional spectra of ϵ_1 for different depths of measurement (1, 36 m; 2, 52 m; 3, 73 m; 4, 90 m; 5, 110 m; 6, 140 m).

the approximating straight line for the range $k\eta = 0.018$–0.120 (between the vertical lines) is -0.44; it corresponds to the mean value $\bar{\mu} = 0.56$, mentioned earlier.

The horizontal variability of $\tilde{\epsilon}$ is shown in Fig. 3. The values of $\tilde{\epsilon}$, calculated from (4), vary by two orders of magnitude over a distance of order 70 m.

Since ϵ is strongly intermittent, its average values, averaged over comparatively short intervals, vary considerably. In this context, one cannot expect to discover definite relationships between the values of $\tilde{\epsilon}$ and the "background" conditions, because hydrographic characteristics, based on standard observations, correspond to much larger averaging scales. Moreover, space-time discrepancies between hydrographic data and fluctuation measurements are inevitable. In order to avoid such discrepancies, one must calculate $\tilde{\epsilon}$ either from very long series of observations or fix the local space-time background conditions.

3. Analysis using structure functions

In a refined theory of locally isotropic turbulence, the statistical characteristics of small-scale turbulence depend on the probability distribution law for ϵ_r. One of the indirect methods for obtaining information on this distribution is by way of structure functions. According to theory, in the inertial subrange, the structure function of order P, averaged over all possible

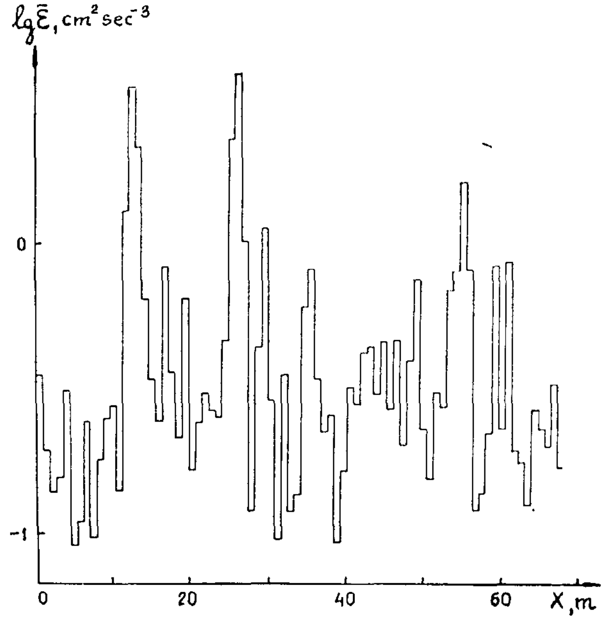

FIG. 3. Space variability of value of ϵ_1 along the line of measurement.

values of ϵ_n (to be denoted by $\langle\ \rangle$) has the form

$$D_P(r)=\overline{(\Delta_r u)^P}=\langle D_P(r,\epsilon_r)\rangle\sim\langle\epsilon^{P/3}\rangle r^{P/3}\sim r^{P/3-\mu_{P/3}}, \quad (6)$$

where $\Delta_r u=u(x+r)-u(x)$, $D_P(r,\epsilon_r)$ is the value of the structure function of order P with constant ϵ_r, $\langle\epsilon_r^{P/3}\rangle \sim r^{-\mu_{P/3}}$ is the statistical moment of order $P/3$ of ϵ_r, and $\mu_{P/3}$ is the correction to the universal laws of locally isotropic turbulence for the structure functions of order P, due to fluctuations in ϵ_r.

The following intermittency model for ϵ_r has been suggested by Yaglom (1966) in the inertial subrange:

$$\mu_{P/3}=\frac{1}{18}P(P-3)\mu. \quad (7)$$

Novikov (1971) has shown that $\mu_{P/3}\leqslant P/3$. He has suggested a particular intermittency model for ϵ_r, according to which

$$\mu_{P/3}=\frac{P}{3}-\log_2\frac{P+3}{3}. \quad (8)$$

In the present paper, high-order structure functions are also investigated, the values of $\mu_{P/3}$ have been calculated and Eqs. (7) and (8) checked for oceanic conditions.

Using initial series of values of longitudinal fluctuating velocities, the following structure functions have been computed, with the exponents following directly from (6):

$$\phi_{1P}(r)=\overline{|\Delta_r u|^P}\sim r^{P/3-\mu_{P/3}} \quad (9a)$$

$$[\phi_{2P}(r)]^{\frac{1}{2}}=[\overline{|\Delta_r u|^{2P}}]^{\frac{1}{2}}\sim r^{P/3-\frac{1}{2}\mu_{2P/3}} \quad (9b)$$

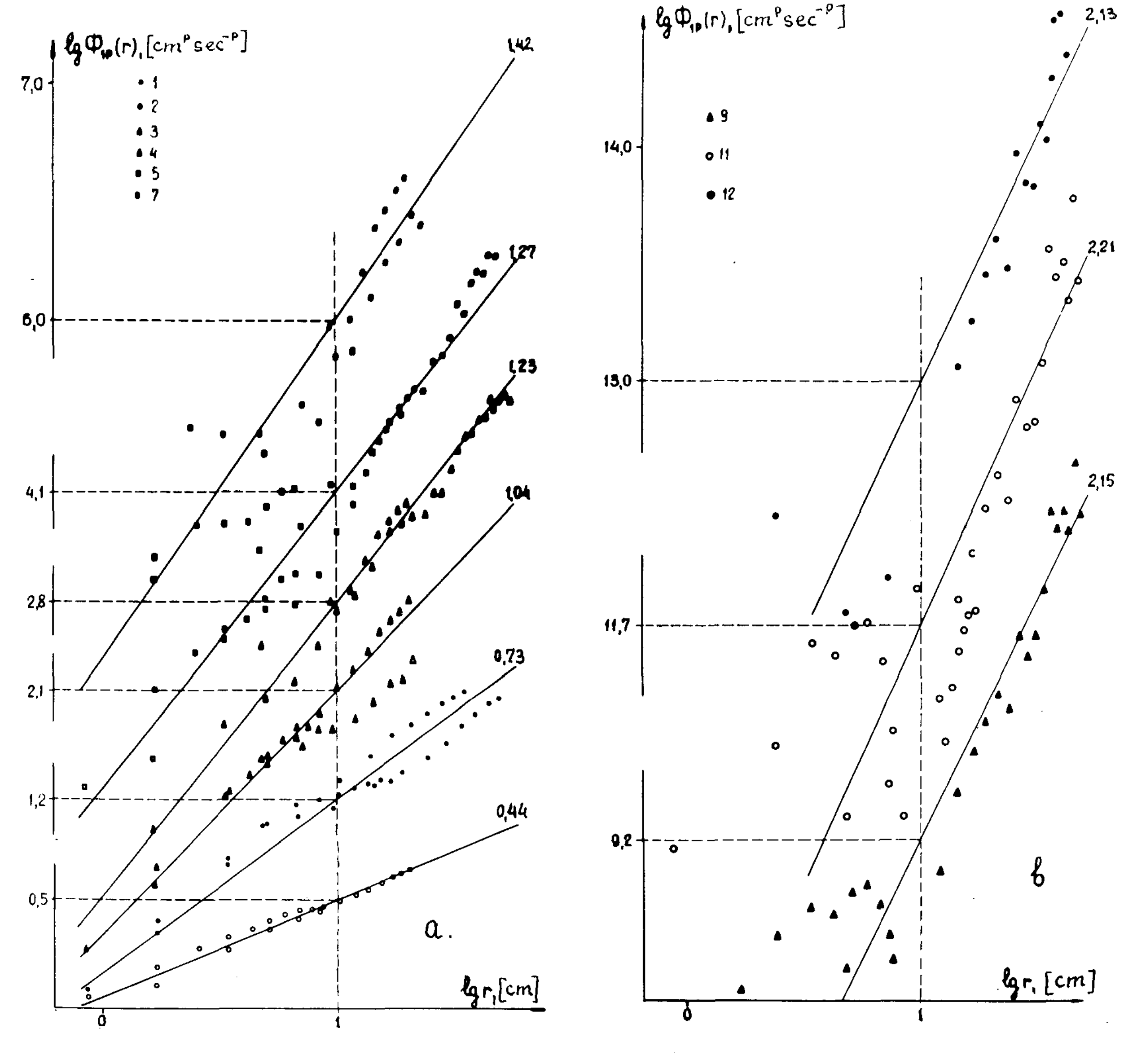

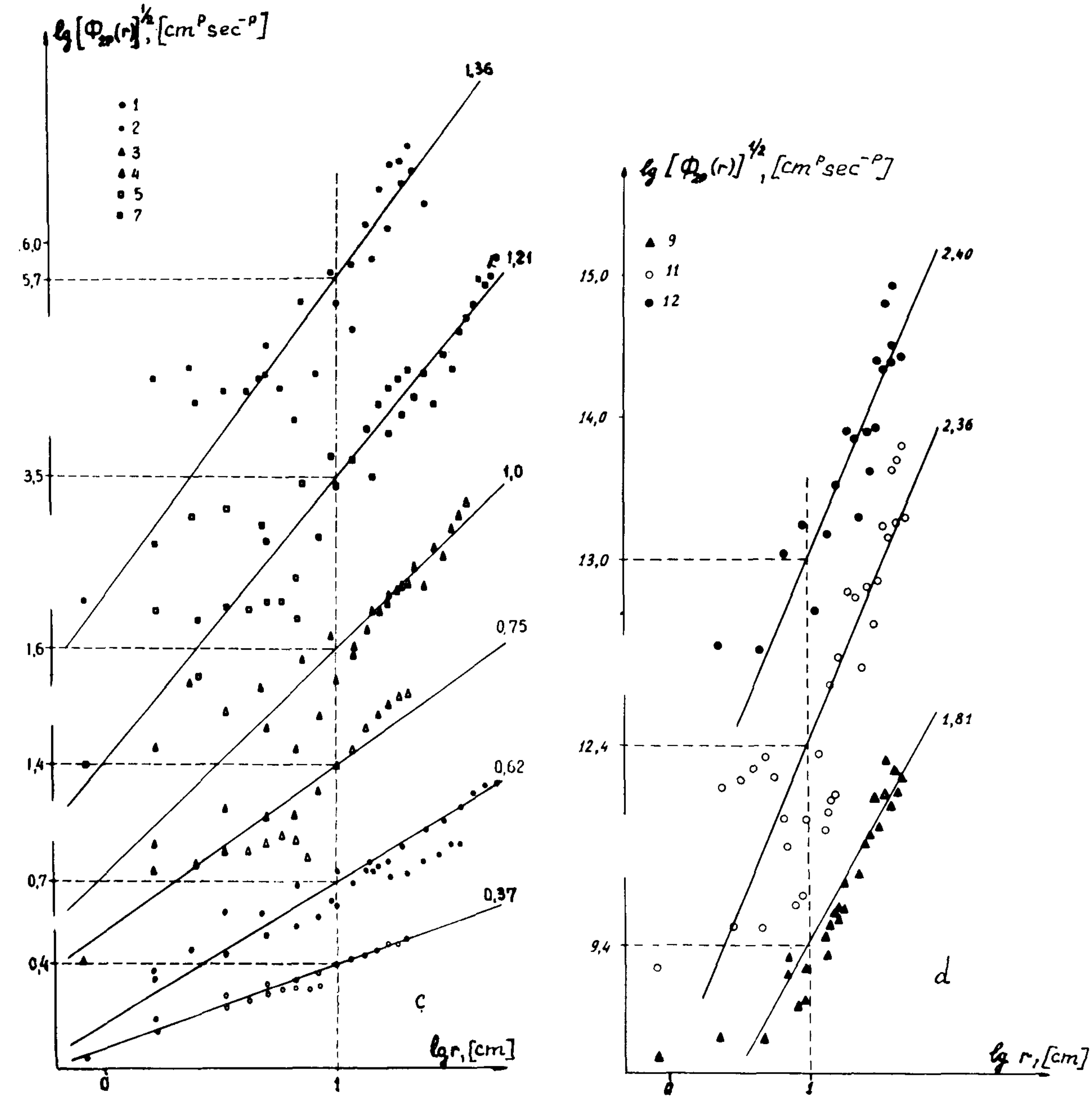

FIG. 4. Structure functions $\phi_{1P}(r)$ (a,b) and $[\phi_{2P}(r)]^{1/2}$ (c,d) of longitudinal velocity fluctuations in the ocean. Different symbols correspond to the values of P, shown in the upper left-hand corner of each figure. The figures on the right ends of the approximating straight lines show its slope.

$$F_{3P}(r)=\frac{\overline{|\Delta_r u|^{3P}}}{[\phi_{2P}(r)]^{\frac{3}{2}}}\sim r^{-\mu_P+\frac{3}{2}\mu_{2P/3}} \qquad (9c)$$

$$F_{4P}(r)=\frac{\overline{|\Delta_r u|^{4P}}}{[\phi_{2P}(r)]^{2}}\sim r^{-\mu_{4P/3}+2\mu_{2P/3}}. \qquad (9d)$$

Due to the presence in the signal of noise of different origin, the slopes of the empirical functions (9) are not always determined with sufficient accuracy, in particular, for large values of P. Nevertheless, as a rule, the graphs obtained permit evaluation, on a logarithmic scale, of the slopes of the functions (9). Hence one may find the values of $\mu_{P/3}$ and discover the character of the relationship between $\mu_{P/3}$ and P.

Fig. 4 presents the graphs of the structure functions $\varphi_{1P}(r)$ and $[\varphi_{2P}(r)]^{\frac{1}{2}}$ for $P=1, 2, 3, 4, 5, 7, 9, 11, 12$, with special symbols for P. The ordinates of the intersections of the approximating straight lines and the vertical straight line through $\log r=1$ characterize

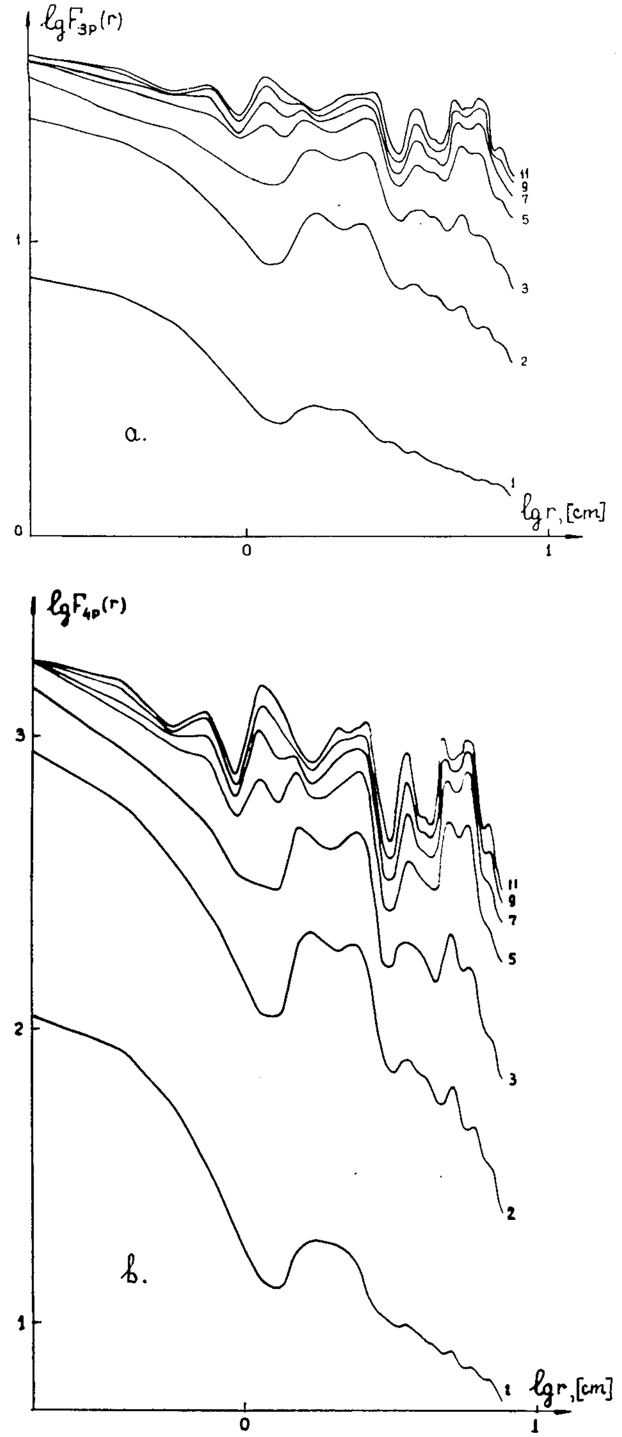

FIG. 5. Non-dimensional structure functions $F_{3P}(r)$ and $F_{4P}(r)$ of the longitudinal velocity fluctuations at a depth of 195 m. The value of P is given at the right-hand end of each curve.

the mean levels of the corresponding structure functions. The slopes of the straight lines yield the values of the powers $\mu_{P/3}$ and $\mu_{2P/3}$.

Fig. 5 presents the graphs of the non-dimensional structure functions $F_{3P}(r)$ and $F_{4P}(r)$ for $P=1, 2, 3, 5, 7, 9, 11$. Using the values of $\mu_{2P/3}$ already calculated through approximating straight lines, not shown on the figure, we determine μ_P and $\mu_{4P/3}$.

Fig. 6 shows the dependence of $\mu_{P/3}$ on P on a logarithmic scale. Our results (shown by the solid circles) are compared with those of different authors for atmospheric measurements. The theoretical curves 1 and 2 correspond to the models of Eqs. (8) and (7), respectively, with $\mu=\mu_2=0.51$. Curves 3 and 4 were calculated from Eq. (7) for $\mu=0.35$ and 0.70. These values of μ correspond to the minimum and maximum values in the work of different authors, obtained by means of the spectrum $E^{(\epsilon)}(k)$ of the random quantity ϵ_r.

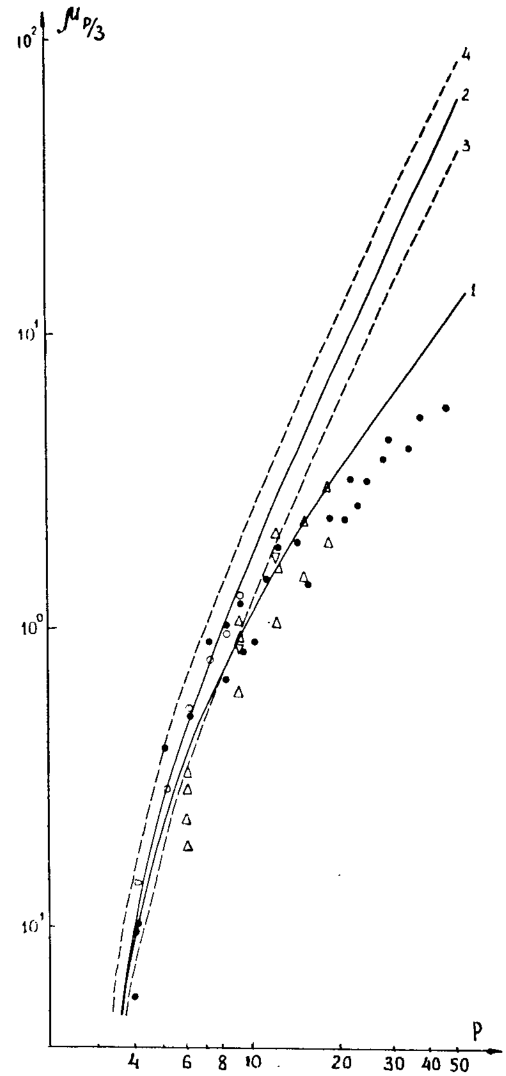

FIG. 6. Variation of $\mu_{p/3}$ with P: theoretical curve 1 calculated according to Eq. (8); and curves 2, 3, 4 according to Eq. (7) for $\mu=0.51$, 0.35, 0.70, respectively. Notation: ●, our data; △, data by Holmyanski (1972, 1973); ▽, data by Stewart *et al.* (1970); ○, data by Van Atta and Park (1972).

The experimental points lie below curve 2 for $P \gtrsim 7$–9. However, since the exact value of μ is still unknown, it is felt that the points lying between curves 3 and 4 correspond to the model of Eq. (7). In this case one can draw the following conclusions concerning the relationship between $\mu_{P/3}$ and P: Eq. (7), proposed by Yaglom, describes satisfactorily this relation in the interval $4 \lesssim P \lesssim 10$–12; for large values of P, the function $\mu_{P/3}$ increases more slowly than predicted by Eq. 7. Eq. 8, proposed by Novikov, approximates better the experimental points in the interval $4 \lesssim P \lesssim 12$–16.

Therefore the results of our evaluation of structure functions of higher orders of the velocity field in the ocean may be indirectly indicative of a confirmation of Novikov's model which assumes that the distribution of probabilities for ϵ_r with decreasing scale r approaches the normal logarithm distribution and the function μ_q satisfies inequality $\mu_q \leqslant \mu - 2 + q$ at $q \geqslant 2$.

REFERENCES

Holmyanski, M. Z., 1972: Measurement of micro-turbulent pulsations of the wind velocity derivative in the near ground layer of the atmosphere. *Izv. Akad. Nauk SSSR, Fys. Atmos. Okeana*, **8**, No. 8, 818–828.

——, 1973: Measurement of the coefficient of breakup of turbulence. *Izv. Akad. Nauk SSSR, Fys. Atmos. Okeana*, **9**, No. 8, 801–812.

Kolmogorov, A. N., 1962: A refinement of previous hypothesis concerning the local structure of turbulence in a viscous incompressible fluid at high Reynolds number. *J. Fluid Mech.*, **13**, 81–85.

Monin, A. S., 1962: On the spectrum of turbulence in an atmosphere with non-homogeneous temperature. *Izv. Akad. Nauk SSSR, Ser. Geofys.*, **3**, 397–407.

Novikov, E. A., 1971: Intermittency and scale similarity in the structure of turbulent flow. *Prikl. Mat. Mekh.*, **35**, No. 2, 266–277.

Obukhov, A. M. 1962: Some specific features of atmospheric turbulence. *J. Fluid Mech.*, **13** (part 1), 77–81.

Stewart, R. W., and H. L. Grant, 1962: Determination of the rate of dissipation of turbulent energy near the sea surface in the presence of waves. *J. Geophys. Res.*, **67**, 3177–3180.

——, J. K. Wilson and R. W. Burling, 1970: Some statistical properties of small scale turbulence in an atmospheric boundary layer. *J. Fluid Mech.*, **41** (part 1), 141–152.

Van Atta, C. W., and J. Park, 1972: Statistical self-similarity and inertial subrange turbulence. Statistical models and turbulence. *Lecture Notes in Physics*, Vol. 12, Springer-Verlag.

Yaglom, A. M., 1966: On the effect of fluctuations of energy dissipation on the form of the turbulence characteristics in the inertial interval. *Dokl. Akad. Nauk SSSR*, **166**, No. 1, 49–52.